Physics Letters B 734 (2014) 345–349

Contents lists available at ScienceDirect

Physics Letters B

www.elsevier.com/locate/physletb

Testing hybrid natural inflation with BICEP2

Mariana Carrillo-González [a], Gabriel Germán [a,*], Alfredo Herrera-Aguilar [b,c], Juan Carlos Hidalgo [a], Roberto A. Sussman [d]

[a] Instituto de Ciencias Físicas, Universidad Nacional Autónoma de México, Apdo. Postal 48-3, 62251 Cuernavaca, Morelos, Mexico
[b] Departamento de Física, Universidad Autónoma Metropolitana Iztapalapa, San Rafael Atlixco 186, CP 09340, México D.F., Mexico
[c] Instituto de Física y Matemáticas, Universidad Michoacana de San Nicolás de Hidalgo, Edificio C-3, Ciudad Universitaria, CP 58040, Morelia, Michoacán, Mexico
[d] Instituto de Ciencias Nucleares, Universidad Nacional Autónoma de México, Apdo. Postal 70-543, 04510 México D.F., Mexico

ARTICLE INFO

Article history:
Received 4 April 2014
Received in revised form 30 April 2014
Accepted 20 May 2014
Available online 27 May 2014
Editor: S. Dodelson

ABSTRACT

We analyse *Hybrid Natural Inflation* in view of the recent results for the tensor index reported by BICEP2. We find that it predicts a large running of the scalar spectrum which is potentially detectable by large scale structure through measurements of clustering of galaxies in combination with CMB data and by 21 cm forest observations. The running of the running is also relatively large becoming close to 10^{-2}. Along the way, we find general consistency relations at which observables are subject if the slow-roll approximation is imposed. Failure to satisfy these equations by the values obtained for the observables in surveys would be a failure of the slow-roll approximation itself.

1. Introduction

There is a considerable interest in the recent results reported by BICEP2 [1]. If confirmed they would give an important boost to the community working in inflationary cosmology since a non-vanishing tensor index $r = 0.2^{+0.07}_{-0.05}$ ($r = 0.16^{+0.06}_{-0.05}$ when foreground subtraction based on dust models has been carried out [1]) is a very distinctive characterisation of inflation [2–8].

In particular, from this data the scale of inflation can be inferred to lie somewhere between 2.03×10^{16} GeV and 2.36×10^{16} GeV, which points at new physics at or beyond the *GUT* scale.

Here we study a model of inflation [9–11], based on a Goldstone (shift) symmetry and in a hybrid mechanism: *Hybrid Natural Inflation* [12]. The original inflationary model based on an anomalous Abelian symmetry is the *Natural Inflation* model of Freese et al. [13–15]. In natural inflation, quantum corrections generate a small mass term for the aspiring Goldstone mode. A potential problem for the model is that, to produce sufficient inflation, the scale of symmetry breaking f must be greater than the Planck scale in which case large quantum gravity corrections could appear.

Hybrid inflation scenarios [16], where the evolution of more than one field is important, have become common within the inflationary paradigm. Thus, *Hybrid Natural Inflation* [12], in which a second field is responsible for terminating inflation, is a well motivated inflationary model. While this model was originally formulated to realise low scales of inflation [17], hybrid natural inflation finds applications beyond this purpose. In hybrid natural inflation the inflaton is a pseudo-Goldstone boson with a small mass due to the rupture of the symmetry at the quantum level or by explicit breaking. Since the end of inflation is triggered by a second field, the number of e-folds of inflation N_χ depends on the auxiliary field χ allowing for a viable model, with values of f at or below the Planck scale.

The goal of this paper is to constrain the free parameters of hybrid natural inflation in light of the data from BICEP2. Along the way, we find general consistency relations at which observables are subject if the slow-roll approximation is imposed. We find, in particular, that hybrid natural inflation can sustain a large scalar running index. The presence of a large running could be a possible resolution to the apparent tension between high values of r and previous indirect limits based on temperature measurements [18]. A large running would introduce a scale into the scalar power spectrum to suppress power on large angular scales [19]. As discussed in [20] the running is potentially detectable by large scale structure through measurements of clustering of high-redshift galaxy surveys in combination with CMB data. High-redshift may also be probed with the 21 cm forest signal which tracks the density field. This could be a powerful proof to observe small-scale power spectrum (SSPS) at $k \geq 10$ Mpc^{-1}. Mass function of collapsed gas in starless minihalos can be very sensitive to the SSPS, thus providing a system for observing effects on the scalar running index. In [21] an analysis is presented where halo

* Corresponding author.
E-mail address: gabriel@fis.unam.mx (G. Germán).

http://dx.doi.org/10.1016/j.physletb.2014.05.062
0370-2693/

mass functions and abundance of 21 cm absorbers are shown for several assumed combinations of the spectral index and running.

Refs. [22] and [23] contain discussions on a ground-based Stage IV CMB experiment, CMB-S4 with $\mathcal{O}(500{,}000)$ detectors by 2020. It is expected that observations with this polarization experiment will probe large angular scales corresponding to low-multipole spectra $1 < l < 100$ and unambiguously detect tensor modes with large r. These next-order measurements will presumably detect deviations in the power-law spectrum, parametrized as

$$n_s(k) = n_s(k_0) + \frac{dn_s}{d\ln k}\ln\left(\frac{k}{k_0}\right) + \cdots. \tag{1}$$

A detection of a non-zero running $\frac{dn_s}{d\ln k}$, through measurements of the E-mode damping tail, could provide information about the inflationary potential or point to models other than inflation.

Our presentation is organised as follows: in Section 2 we determine general constraint equations among the observables based on the slow-roll paradigm. These constraints make no use of the specific form of the potential. Failure to satisfy these equations by the values obtained for the observables in surveys would be a failure of the slow-roll approximation itself. Section 3 presents a discussion of natural inflation in light of the BICEP2 data. Following this line of presentation we then generalise results for hybrid natural inflation where f is not restricted by the number of e-folds. Finally we summarise our results and conclude in Section 4.

2. Slow-roll parameters, observables and model independent results

One can set constraints on the parameters of a given inflationary potential by imposing the requirement of acceptable inflation in terms of slow-roll parameters. This then leads to the determination of observables produced by that potential. The usual slow-roll parameters [24] which involve the potential and its derivatives are

$$\epsilon \equiv \frac{M^2}{2}\left(\frac{V'}{V}\right)^2, \qquad \eta \equiv M^2\frac{V''}{V}, \qquad \xi_2 \equiv M^4\frac{V'V'''}{V^2},$$
$$\xi_3 \equiv M^6\frac{V'^2V''''}{V^3}, \tag{2}$$

where primes denote derivatives with respect to ϕ. M is the reduced Planck mass $M = 2.44\times 10^{18}$ GeV and we set $M = 1$ in what follows. In the slow-roll approximation the observables are given in terms of the usual slow-roll parameters [24] as follows

$$n_t = -2\epsilon = -\frac{r}{8}, \tag{3}$$

$$n_s = 1 + 2\eta - 6\epsilon, \tag{4}$$

$$n_{tk} = \frac{dn_t}{d\ln k} = 4\epsilon(\eta - 2\epsilon), \tag{5}$$

$$n_{sk} = \frac{dn_s}{d\ln k} = 16\epsilon\eta - 24\epsilon^2 - 2\xi_2, \tag{6}$$

$$n_{skk} = \frac{d^2n_s}{d\ln k^2} = -192\epsilon^3 + 192\epsilon^2\eta - 32\epsilon\eta^2 - 24\epsilon\xi_2 + 2\eta\xi_2 + 2\xi_3, \tag{7}$$

$$\delta_H^2(k) = \frac{1}{150\pi^2}\frac{\Lambda^4}{\epsilon_H}, \tag{8}$$

where n_t is the tensor spectral index, r is the usual tensor index or the ratio of tensor to scalar perturbations, n_{tk} the running of the tensor index, n_s the scalar spectral index, n_{sk} its running, n_{skk} the running of the running, in a self-explanatory notation. The density perturbation at wave number k is $\delta_H^2(k)$ and Λ is the scale of inflation with $\Lambda \equiv V_H^{1/4}$. Note that all these quantities are described in terms of the inflaton scale ϕ_H, at which the perturbations are produced, some 50–60 e-folds before the end of inflation. Defining the quantity δ_{ns} by $\delta_{ns} \equiv 1 - n_s$ we note that Eq. (5) can be written as a constraint equation among the observables

$$n_{tk} = \frac{r}{64}(r - 8\delta_{ns}). \tag{9}$$

More constraint equations can be written as above but they have little chance of being falsified in the near future [25]. Note that Eq. (9) is a model independent constraint on the observables and should be satisfied by *any* model of inflation based on the slow-roll paradigm. Failure to satisfy this equation by the values obtained for the observables in surveys would indicate a departure from the slow-roll approximation itself. As a simple numerical example we see that the reported values $\delta_H = 1.87\times 10^{-5}$, $\delta_{ns} \equiv 1 - n_s = 1 - 0.96 = 0.04$, and, $0.15 < r < 0.27$ yield $-4\times 10^{-4} < n_{tk} < -2.1\times 10^{-4}$. The values also set the scale of inflation in the range 2.03×10^{16} GeV $< \Lambda < 2.36\times 10^{16}$ GeV. We stress that these values for n_{tk} and Λ are *model independent*. They only depend on the values given to δ_H, n_s, r *and* the validity of the slow-roll approximation.

Thus, according to the slow-roll approximation for single field inflation we are predicting that n_{tk} will take values within the range $-4\times 10^{-4} < n_{tk} < -2.1\times 10^{-4}$.

On the other hand, the equation for the running Eq. (6) can be written as

$$n_{sk} = \frac{1}{32}\left(3r^2 - 16r\delta_{ns} - 64\xi_2\right). \tag{10}$$

Thus, a determination of n_{sk} would be equivalent to a determination of the parameter ξ_2. In hybrid natural inflation as well as in natural inflation, n_{sk} is given by

$$n_{sk} = \frac{r}{32}\left(3r - 16\delta_{ns} + \frac{8}{f^2}\right), \tag{11}$$

where f is the scale of the (Goldstone) symmetry breaking. A determination of n_{sk} would be a determination of f and, thus, a possible indication of new physics at or beyond the *GUT* scale.

3. Testing hybrid natural inflation

We begin with a brief discussion of natural inflation which is then generalised to hybrid natural inflation. Natural inflation is a single scalar field model, where the end of inflation is determined by the steepening of the potential until $\epsilon = 1$. Thus, the inflaton value at the end of inflation, ϕ_e, is precisely determined and, up to an uncertainty about the number of intermediate e-folds of inflation, so is the inflaton value of the observable scales ϕ_H. As a result natural inflation has only two free parameters: the scale of inflation $\Lambda \equiv V_H^{1/4}$ and f. The natural inflation potential is given by

$$V(\phi) = V_0\left(1 + \cos\left(\frac{\phi}{f}\right)\right) \equiv V_0(1 + c_\phi), \tag{12}$$

where we conveniently have defined $c_\phi \equiv \cos(\frac{\phi}{f})$. From (4) we find that the spectral index is always less than one: $n_s = 1 - \frac{1}{4}(r + (\frac{2}{f})^2)$. Thus, f is determined if we know n_s and r and is given by

$$f = \frac{2}{\sqrt{4\delta_{ns} - r}}. \tag{13}$$

From the reality condition of f, we find a bound on r

Table 1
Numerical values of observables derived for the natural inflation and hybrid natural inflation models specified by Eqs. (12) and (16) respectively. While in natural inflation there is a constraint for $r < 4\delta_{ns} \approx 0.16$ (see Eqs. (14)), hybrid natural inflation is able to accommodate all values of r reported by BICEP2. The quantity N_χ in hybrid natural inflation corresponds to the number of e-folds and its value is controlled by a waterfall field χ to provide the required amount of inflation. The first and fourth rows contain results for the reported case [1] $r = 0.16^{+0.06}_{-0.05}$ with foreground subtraction based on dust models. The case when $r = 4\delta_{ns} \approx 0.16$ is shown in the third and sixth rows, this value corresponds to a minimum of n_{tk} according to Eq. (9). Note also the double-value character of n_{tk}.

	f	a	n_s	r	n_{sk}	n_{skk}	n_{tk}	Λ (GeV)	N
NI	8.9	–	0.96	0.11	-7.2×10^{-4}	-2.9×10^{-5}	-3.6×10^{-4}	1.88×10^{16}	51
NI	20	–	0.96	0.15	-8.0×10^{-4}	-3.2×10^{-5}	-4.0×10^{-4}	2.04×10^{16}	50
NI	∞	–	0.96	0.16	–	–	–	–	–
HNI	1	0.117	0.96	0.11	2.6×10^{-2}	2.2×10^{-3}	-3.6×10^{-4}	1.88×10^{16}	N_χ
HNI	1	0.136	0.96	0.15	3.7×10^{-2}	3.6×10^{-3}	-4.0×10^{-4}	2.04×10^{16}	N_χ
HNI	1	0.140	0.96	0.16	3.9×10^{-2}	4.0×10^{-3}	-4.0×10^{-4}	2.07×10^{16}	N_χ
HNI	1	0.156	0.96	0.20	5.0×10^{-2}	5.8×10^{-3}	-3.8×10^{-4}	2.19×10^{16}	N_χ
HNI	1	0.181	0.96	0.27	6.9×10^{-2}	9.8×10^{-3}	-2.1×10^{-4}	2.36×10^{16}	N_χ

$$r < 4\delta_{ns} \approx 0.16, \tag{14}$$

which is just within the range reported by BICEP2. As an example we calculate f from Eq. (13) in the case when $\delta_{ns} \equiv 1 - n_s = 1 - 0.96 = 0.04$ and $r = 0.15$. For these values one gets $f \approx 20$ and

$$N \approx 50, \qquad \Lambda \approx 2 \times 10^{16}\ \text{GeV}, \qquad n_{tk} \approx -4 \times 10^{-4},$$
$$n_{sk} \approx -8 \times 10^{-4}, \qquad n_{skk} \approx -2 \times 10^{-5}. \tag{15}$$

We see that natural inflation is marginally able to accommodate the data reported by BICEP2. The price to pay is a very large symmetry breaking scale f, with $f = 20$. In Table 1 we compare these values with other models and with results for the reported case $r = 0.16^{+0.06}_{-0.05}$ when foreground subtraction based on dust models has been carried out [1].

We now investigate whether hybrid natural inflation is able to lower the value of f while, at the same time, keeping reasonable values for the observables. As discussed in [12], the terms of the (hybrid) inflaton potential relevant when density perturbations are being produced have a simple universal form corresponding to the slow-roll of a single inflaton field ϕ:

$$V \simeq V_0\left(1 + a\cos\left(\frac{\phi}{f}\right)\right) = V_0(1 + ac_\phi). \tag{16}$$

Natural inflation corresponds to the case $a = 1$ while hybrid natural inflation demands $a < 1$ [17]. The slow-roll parameters for this model are given by

$$\epsilon = \frac{1}{2}\left(\frac{M}{f}\right)^2 a^2 \frac{1 - c_\phi^2}{(1 + a\,c_\phi)^2}, \tag{17}$$

$$\begin{aligned}\eta &= -\left(\frac{M}{f}\right)^2 a\,\frac{c_\phi}{1 + a\,c_\phi} \\ &= \left(\frac{M}{f}\right)^2 \frac{a^2}{(1-a^2)}\left(1 \pm \frac{1}{a}\sqrt{1 - \frac{2(1-a^2)f^2}{a^2}\epsilon}\right),\end{aligned} \tag{18}$$

$$\xi_2 = -\left(\frac{M}{f}\right)^4 a^2 \frac{1 - c_\phi^2}{(1 + a\,c_\phi)^2} = -2\left(\frac{M}{f}\right)^2 \epsilon, \tag{19}$$

$$\xi_3 = \left(\frac{M}{f}\right)^6 a^3 \frac{1 - c_\phi^2}{(1 + a\,c_\phi)^3} c_\phi = -2\left(\frac{M}{f}\right)^2 \epsilon\eta. \tag{20}$$

From Eqs. (4) and (18) we get an expression for f

$$f = \frac{4a}{(r(1-3a^2) + 8a^2\delta_{ns} + \sqrt{4a^2(4\delta_{ns} - r)^2 + r^2(1-a^2)})^{1/2}}. \tag{21}$$

It is easy to check that the reality condition for f is always satisfied provided $a < 1$. When $r \leq 4\delta_{ns}$, Eq. (21) reduces to the natural inflation formula Eq. (13) in the limit $a \to 1$. However Eq. (21) is more general, valid for $r \geq 4\delta_{ns}$, including all relevant values of r reported by BICEP2.

Apart from Eq. (18), Eqs. (17) to (20) look the same as in the natural inflation case with $a = 1$. From Eqs. (3), (4), (19) and (20), one can see that the expression for n_{sk} and n_{skk} can be respectively written as

$$n_{sk} = \frac{r}{32}\left(3r - 16\delta_{ns} + \frac{8}{f^2}\right), \tag{22}$$

$$n_{skk} = \frac{r}{128}\left(3r^2 + \frac{12}{f^2}r - \left(2\delta_{ns} - \frac{1}{f^2}\right)32\delta_{ns}\right). \tag{23}$$

When f is of order $\mathcal{O}(1)$, the running can simply be written as

$$n_{sk} \approx \frac{r}{4f^2}, \tag{24}$$

thus, n_{sk} behaves like a simple scaled function of the tensor index. From Eq. (22) we get

$$f = \left(\frac{8r}{32n_{sk} - r(3r - 16\delta_{ns})}\right)^{1/2}. \tag{25}$$

One can easily find bounds for n_{sk}, these are

$$n_{sk} \geq -9 \times 10^{-4} \quad \text{for } r \geq 0.15, \tag{26}$$

$$n_{sk} > 0 \quad \text{for } r > \frac{16}{3}\delta_{ns} \approx 0.21. \tag{27}$$

While natural inflation can only accommodate small negative values of n_{sk}, hybrid natural inflation allows also for positive values of n_{sk}. In Table 1 we show some of the observables using values for r reported by BICEP2. Note that in hybrid natural inflation f is any positive number restricted only by the lower value of the scale of inflation Λ. From the expression for the running, Eq. (22), one can see that small values of f would imply unacceptably large n_{sk} while large f could give negligible contribution to the running. The lack of a theory of quantum gravity makes the contemplation of a scale f above the Planck scale a mere speculation.

Figs. 1 and 2 show the running of the spectral index n_{sk}, Eq. (22) and the running of the running n_{skk}, Eq. (23), respectively as functions of f and r for the entire range of r-values reported by BICEP2. In both cases the left figures show positive n_{sk} and n_{skk} for small values of f (in particular for $f < 1$) while, for large f both observables can become negative (right). The negative section of the figure is highlighted by the level curve at $n_{sk} = 0$, $n_{skk} = 0$, respectively.

Within hybrid natural inflation there is a maximum value that the tensor index can acquire. From Eq. (18) follows that

$$\epsilon = \frac{a^2}{2f^2} + a^2\eta - \frac{(1-a^2)f^2}{2}\eta^2, \tag{28}$$

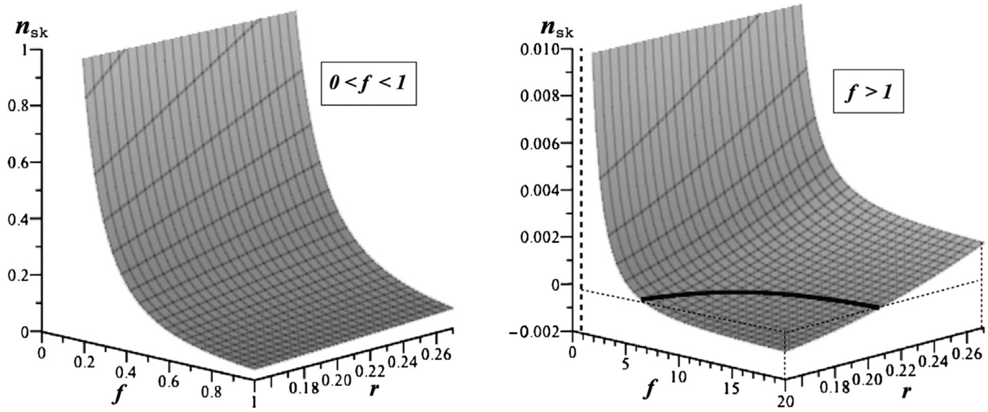

Fig. 1. The running of the spectral index $n_{sk} \equiv \frac{dn_s}{d\ln k}$, Eq. (22) is here shown as a function of the tensor index r and the scale of Goldstone symmetry breaking f with $\delta_{ns} \equiv 1 - n_s = 1 - 0.96 = 0.04$. The left panel shows that n_{sk} is always positive for small values of f (in particular for $f < 1$) while, for large f it can become negative (right panel). The negative section of the figure is highlighted by the level curve at $n_{sk} = 0$. The presence of a large running in hybrid natural inflation could be a possible resolution to the apparent tension between high values of r and previous indirect limits based on temperature measurements [18].

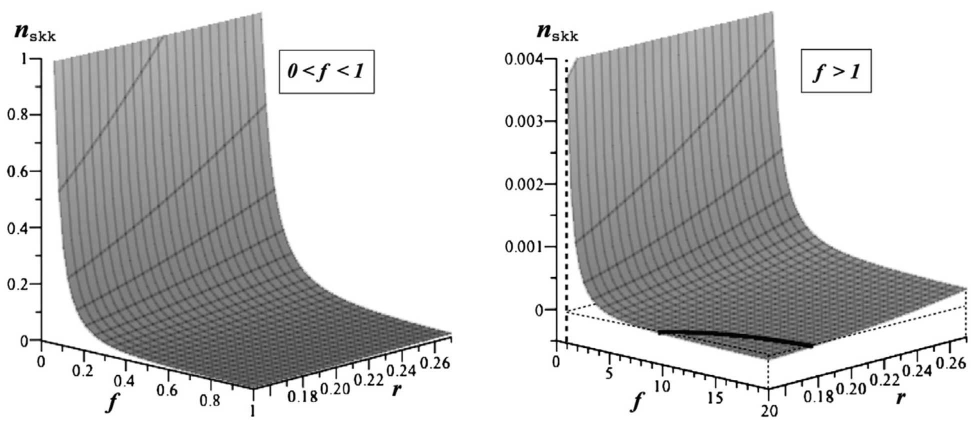

Fig. 2. The running of the running $n_{skk} \equiv \frac{d^2 n_s}{d\ln k^2}$, Eq. (23) is shown as a function of the tensor index r and the symmetry breaking scale f with $\delta_{ns} \equiv 1 - n_s = 1 - 0.96 = 0.04$. The left panel shows that n_{skk} is always positive for small values of f while, for large f it can become negative (right panel). The negative section of the figure is highlighted by the level curve at $n_{skk} = 0$. From Table 1 we see that the running of the running can be high and very close to 10^{-2}.

note that in the case $a = 1$, as in natural inflation, this function is monotonous. In general $\epsilon(\eta)$ presents a maximum where $\eta = 2\epsilon$, located at

$$\cos\left(\frac{\phi_{\max}}{f}\right) = -a. \tag{29}$$

Contrary to initial expectations [26] the maximum of r (see Eq. (17)) is not located at $\phi/f = \pi/2$ but at $\phi_{\max}/f = \cos^{-1}(-a)$ and is given by

$$r_{\max} = 8\delta_{ns}. \tag{30}$$

If the maximum occurred in the observable scales, i.e., if $\phi_{\max} = \phi_H$ then $r_{\max} = 8\delta_{ns} \approx 0.32$. This value of $r_{\max}$ is larger than the maximum value $r = 0.27$ reported by BICEP2. The simple plot of r versus ϕ in Fig. 3 shows that the values reported by BICEP2 are such that (within hybrid natural inflation) $\phi_{\text{BICEP2}} < \phi_{\max}$, thus, r grows up from ϕ_{BICEP2} values to the maximum and then decreases again to ϕ_{BICEP2} values but with the spectral index now larger than 0.96.[1] Thus, during the evolution of ϕ from ϕ_H to the end of inflation at ϕ_e, the inflationary period always contains $\phi_{\max}$, and thus $r_{\max}$.

Independently of the hybrid natural inflation case, Eq. (30) can in fact be generalised further to a critical point; the resulting value $r_{\text{critical}} = 8\delta_{ns}$ is then a universal result [25].

4. Summary and conclusions

We find that hybrid natural inflation can accommodate the recent results for the tensor index reported by BICEP2 with values $\mathcal{O}(M_{\text{Planck}})$ of the symmetry breaking scale f while keeping reasonably small values for the other observables. From Table 1 we see that natural hybrid inflation predicts a relatively large value for the running n_{sk} which could be observable in the near future. The presence of a large running could be a possible resolution to the apparent tension between high values of r and previous indirect limits based on temperature measurements. A large running would introduce a scale into the scalar power spectrum to suppress power on large angular scales. The running is potentially detectable by large scale structure through measurements of clustering of high-redshift galaxy surveys in combination with CMB data. High-redshift may also be probed with the 21 cm forest signal observations. Again from Table 1 we see that the running of the running can also be large becoming close to 10^{-2}.

We have also shown that in the context of single field inflation based on the slow-roll paradigm there are equations constraining the observables which make no use of any specific potential. In particular, failure to satisfy Eq. (9) by values obtained for the ob-

[1] The possibility of a blue spectrum as a result of the running of the spectral index allows for the overproduction of primordial black holes [27]. This aspect will be explored in detail elsewhere

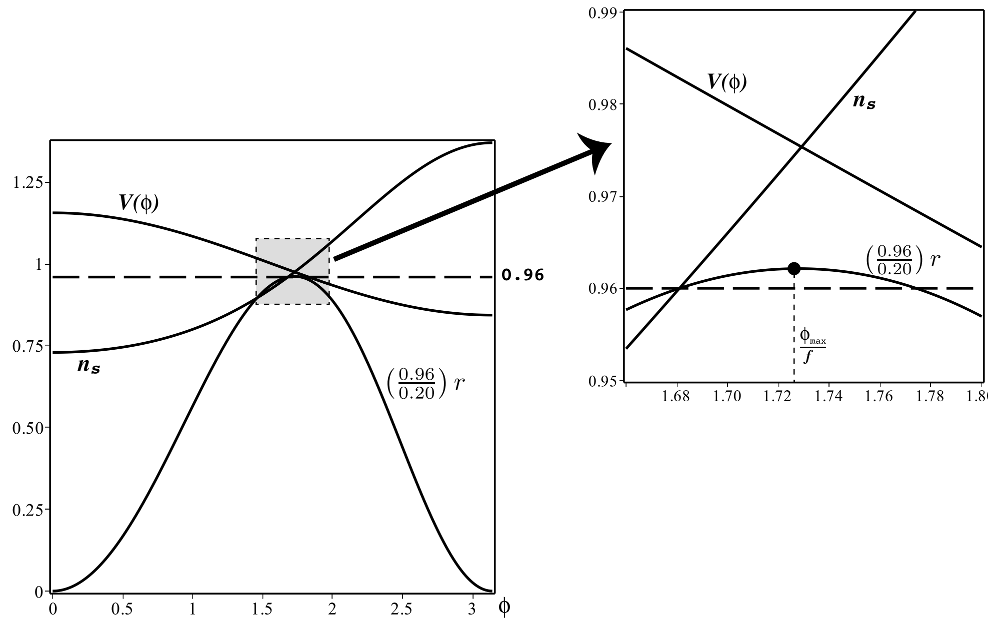

Fig. 3. The plot and inset show the values of the normalised potential V/V_0, spectral index n_s and a rescaled tensor index r in the hybrid natural inflation model. Values reported by BICEP2 are such that $\phi_{\mathrm{BICEP2}} < \phi_{\max}$, thus, r grows from ϕ_{BICEP2} values to the maximum and then decreases again to ϕ_{BICEP2} values but with the spectral index then larger than 0.96. In the figure we use the set of values coming from the Table 1 where $f = 1$, $a = 0.156$, to obtain $n_s = 0.96$, $r = 0.20$, etc. Thus, the evolution of ϕ during the inflationary period from ϕ_{H} to the end of inflation at ϕ_e always contains $\phi_{\max}$ where r reaches a maximum value $r_{\max}$ before starting to decrease. Consequently far more e-folds are generated near the end of inflation (where r is small) rather than close to ϕ_{H}.

servables in surveys would indicate a departure from the slow-roll approximation itself.

Acknowledgements

We gratefully acknowledge support from *Programa de Apoyo a Proyectos de Investigación e Innovación Tecnológica* (PAPIIT) UNAM, IN103413-3, *Teorías de Kaluza–Klein, inflación y perturbaciones gravitacionales* and IA101414-1, *Fluctuaciones no-lineales en cosmología relativista*. A.H.A. is grateful to the staff of ICF, UNAM and UAM-Iztapalapa for hospitality. M.C.G. acknowledges a scholarship from DGAPA-UNAM, IN103413-3. R.A.S. acknowledges finantial support from grant CONACYT 132132. G.G., A.H.A., J.C.H. and R.A.S. thank SNI, 10613 for support.

References

[1] P.A.R. Ade, et al., BICEP2 Collaboration, arXiv:1403.3985 [astro-ph.CO].
[2] Alex Kehagias, Antonio Riotto, arXiv:1403.4811.
[3] Katherine Freese, William H. Kinney, arXiv:1403.5277.
[4] Cheng Cheng, Qing-Guo Huang, arXiv:1403.5463.
[5] Sayantan Choudhury, Anupam Mazumdar, arXiv:1403.5549.
[6] Luis E. Ibanez, Irene Valenzuela, arXiv:1403.6081.
[7] Camille Bonvin, Ruth Durrer, Roy Maartens, arXiv:1403.6768.
[8] Cheng Cheng, Qing-Guo Huang, arXiv:1403.7173.
[9] A.H. Guth, Phys. Rev. D 23 (1981) 347.
[10] A.D. Linde, Phys. Lett. B 108 (1982) 389.
[11] A. Albrecht, P.J. Steinhardt, Phys. Rev. Lett. 48 (1982) 1220.
[12] G.G. Ross, G. Germán, Phys. Lett. B 684 (2010) 199–204, arXiv:0902.4676 [hep-ph];
G.G. Ross, G. Germán, Phys. Lett. B 691 (2010) 117–120, arXiv:1002.0029 [hep-ph].
[13] K. Freese, J.A. Frieman, A.V. Olinto, Phys. Rev. Lett. 65 (1990) 3233.
[14] F. Adams, J.R. Bond, K. Freese, J.A. Frieman, A.V. Olinto, Phys. Rev. D 47 (1993) 426–455.
[15] K. Freese, C. Savage, W.H. Kinney, Int. J. Mod. Phys. D 16 (2008) 2573, arXiv:0802.0227 [hep-ph].
[16] A. Linde, Phys. Rev. D 49 (1994) 748;
Other general references for hybrid inflation are: D.H. Lyth, A. Riotto, Phys. Rep. 314 (1999) 1, arXiv:hep-ph/9807278;
A.D. Linde, Lect. Notes Phys. 738 (2008) 1, arXiv:0705.0164 [hep-th];
M. Shaposhnikov, J. Phys. Conf. Ser. 171 (2009) 012005.
[17] G. Germán, G.G. Ross, S. Sarkar, Nucl. Phys. B 608 (2001) 423, arXiv:hep-ph/0103243;
G. Germán, G.G. Ross, S. Sarkar, Phys. Lett. B 469 (1999) 46–54,1999, arXiv:hep-ph/9908380.
[18] P.A.R. Ade, et al., Planck Collaboration, arXiv:1303.5082 [astro-ph.CO].
[19] V. Miranda, W. Hu, P. Adshead, arXiv:1403.5231 [astro-ph.CO].
[20] P. Adshead, R. Easther, J. Pritchard, A. Loeb, J. Cosmol. Astropart. Phys. 1102 (2011) 021, arXiv:1007.3748 [astro-ph.CO].
[21] H. Shimabukuro, K. Ichiki, S. Inoue, S. Yokoyama, arXiv:1403.1605 [astro-ph.CO].
[22] K.N. Abazajian, K. Arnold, J. Austermann, B.A. Benson, C. Bischoff, J. Bock, J.R. Bond, J. Borrill, et al., arXiv:1309.5381 [astro-ph.CO].
[23] K.N. Abazajian, K. Arnold, J. Austermann, B.A. Benson, C. Bischoff, J. Bock, J.R. Bond, J. Borrill, et al., arXiv:1309.5383 [astro-ph.CO].
[24] A.R. Liddle, D.H. Lyth, Cosmological Inflation and Large-Scale Structure, Cambridge University Press, 2000.
[25] Mariana Carrillo-González, Gabriel Germán, Alfredo Herrera-Aguilar, Juan Carlos Hidalgo, Roberto A. Sussman, manuscript in preparation expanding the results of version one in arXiv:1404.1122v1 [astro-ph.CO].
[26] Arthur Hebecker, Sebastian C. Kraus, Alexander Westphal, Phys. Rev. D 88 (2013) 123506, arXiv:1305.1947 [hep-th].
[27] K. Kohri, D.H. Lyth, A. Melchiorri, J. Cosmol. Astropart. Phys. 0804 (2008) 038, arXiv:0711.5006 [hep-ph].